Available online at www.sciencedirect.com
SCIENCE DIRECT®
Polymer 45 (2004) 2853–2862
polymer
www.elsevier.com/locate/polymer

Solution properties of nafion in methanol/water mixture solvent

Su-Jen Lee[a], T. Leon Yu[a,b,*], Hsiu-Li Lin[a,b], Wen-Horng Liu[a], Chen-Lan Lai[a]

[a]*Department of Chemical Engineering, Yuan Ze University, Nei-Li, Taoyuan 32026, Taiwan*
[b]*Fuel Cell Center, Yuan Ze University, Nei-Li, Taoyuan 32026, Taiwan*

Received 30 March 2003; received in revised form 15 December 2003; accepted 30 January 2004

Abstract

Dilute solution properties of Nafion in methanol/water (4/1 wt ratio) mixture solvent with Nafion concentrations ranging from 0.2 to 9.0 mg/ml was studied using membrane osmometer, viscoelasticity analyzer, and dynamic light scattering. Two aggregation processes were observed. The primary aggregation process causes formation of smaller sizes ($\sim 10^3$ nm) rod-like aggregation particles, which can be dissociated into single molecular chains by dissolving Nafion in propanol/water mixture solvents, is attributed to the hydrophobic interaction of fluorocarbon backbone. The secondary aggregation process causes formation of larger aggregation particles ($\sim 10^4$ nm), which can be dissociated into primary aggregation particles by mixing NaCl salt into Nafion/methanol/water solutions, is attributed to the ionic aggregation of primary aggregation particles which arise from the electrostatic attraction of Nafion side chain $-SO_3^-$ ion pairs. Two critical concentrations were observed in this concentration regime, i.e. C^* ~around 1.0 mg/ml and C^{**} ~around 5.0 mg/ml in the present study, where transitions of Nafion aggregation conformations occur. C^* is the concentration at which most of the Nafion primary rod-like perfluoro backbone aggregation particles aggregate to form secondary ionic aggregations. C^{**} is the concentration at which the disordered segments of primary aggregation particles start to overlap and self-assemble.

Keywords: Nafion solutions; Dynamic light scattering; Viscoelasticity

1. Introduction

The ionomers known as Nafion are produced by Du Pont and consist of a perfluororinated backbone and ether side chains terminated with sulfonic groups $-SO_3^-$ [1,2]. Nafion membranes have unique properties with respect to stability, solubility, and ionic conductivity, which make them suitable for a variety of applications [3]. In the beginning, Nafion was most often used in electrochemical industry. However, from the mid-1980s, Nafion membrane was found to be an excellent material and a core part of a fuel cell to separate the fuel and oxidant and to transport proton from anode to cathode. Nafion is also used in the solution form for casting into the electrode-membrane assembly (EMA), because a fuel cell electrode transports both ions and electrons [4,5]. Because of the stringent call for a cleaner environment, fuel cell is considered as one of the most important sources of clean energy, and thus Nafion has attracted great attention in both academic and industrial research. An important step in the modification of Nafion membranes is the so-called recast process, in which a film is formed after evaporating the solvent from an ionomer solution. For a fundamental understanding of this process, detailed knowledge of the solution properties is a prerequisite.

The chemical structure of Nafion composes tetrafluoroethylene and sulfonated vinyl ether comonomer. The hydrophobic fluorocarbon component and the hydrophilic ionic groups are incompatible. It is, therefore, not surprising that a degree of phase separation occurs, leading to the formation of interconnected, hydrated ionic clusters which determine the electrochemical properties of the polymer. Dual cohesive energy densities have been observed by swelling measurements [6]. One of the cohesive energy densities is ascribed to the organic fluorocarbon part of the polymer, whereas the other is tentatively attributed to the ionic clusters. The fluorocarbon phase controls the swelling and prevents the ionic phase from dissolving. As the temperature is increased, the fluorocarbon phase melts and permits the ionic phase to dissolve in a mixture of alcohol

* Corresponding author. Address: Department of Chemical Engineering, Yuan Ze University, Nei-Li, Taoyuan 32026, Taiwan. Tel.: +886-3-4638833x553; fax: +886-3-4559373.
E-mail address: cetlyu@saturn.yzu.edu.tw (T.L. Yu).

0032-3861/$ - see front matter © 2004 Elsevier Ltd. All rights reserved.
doi:10.1016/j.polymer.2004.01.076

and water. If the solvent of a Nafion solution is evaporated at room temperature, the morphology of the discontinuous fluorocarbon phase is largely preserved. Such a film is weak and will be redissolved in alcohol. If, however, the solvent is evaporated hot or if the cast film is heated to 100–120 °C, the dispersed fluorocarbon phase will to some extent fuse together and the film will become insoluble.

Numerous studies have been devoted to the structure of perfluorinated ionomer membranes [7–12]. Comparing to the membrane structure of Nafion, however, little is known about the nature and structure of Nafion solutions. Small angle neutron scattering (SANS), small angle X-ray scattering (SAXS) (with Nafion concentration ranging from 5 to 20 wt%) and electron spin resonance (ESR) (with Nafion concentration ranging from 1 to 22 wt%) experiments have given a first insight into the structure of these colloid solutions [13–16]. These experimental results favor the compact cylinder model, in which the solvent-polymer contact is at the surface of the *micelle*, rather than the open coil model, in which the solvent-polymer contact is maintained all along the chain. The Ubbelohde viscosity measurements of dilute solutions of Nafion in aliphatic alcohols exhibited an increase in the reduced viscosity with dilution [17]. This effect increases with the dielectric constant of alcohols. Dynamic light scattering (DLS) experiments were carried out both in 10 mg/ml Nafion/ethanol/water (50/50 vol ratio) [18] and 5.3 mg/ml Nafion/water solutions [19]. Two different sizes of Nafion aggregates were found in both solutions. These authors attributed these aggregates to the hydrophobic interaction of fluorocarbon backbone and the electrostatic attraction through the side chain sulfonic ion pairs.

Most of the commercial Nafion solutions are prepared and dissolved in methanol/water mixture solvents. In the present work, using membrane osmometer, viscoelasticity analyzer, static light scattering (SLS), and DLS, we report the aggregation behavior of Nafion in methanol/water (wt ratio 4/1) mixture solvents with Nafion concentrations ranging from 0.2 to 9.0 mg/ml. It is proposed that Nafion molecules aggregate and form primary compact cylinder particles through hydrophobic interaction of fluorocarbon backbone with ionic side chains locating around the periphery of cylinders, these primary cylinder particles can aggregate again through ionic side chains and form larger secondary aggregation particles with solvent inside the center of aggregation particles [15]. In the present study, we show the primary aggregation cylinder particles can be dissolved into single molecules by dissolving Nafion in propanol/water mixture solvent and the secondary ionic aggregation particles can be dissociated into primary cylinder aggregation particles by adding NaCl salt into Nafion/methanol/water solutions. These results provide evidence that the primary aggregation is due to the hydrophobic fluorocarbon backbone interaction, and the secondary aggregation is due to the electrostatic attraction through the side chain sulfonic ion pairs. In this study, we also reported two critical concentrations, i.e. a lower critical concentration C^* around 1.0 mg/ml and a higher critical concentration C^{**} around 5.0 mg/ml, where transitions of Nafion aggregation conformations occur.

2. Experimental

2.1. Materials

Nafion solution with an equivalent weight of 1100 was purchased from Aldrich Chemical Co (cat no. 27470-4). Nafion resin solution was supplied in H^+ form, which contains 5 wt% of Nafion and 95 wt% of aliphatic alcohol and water solvent mixture.

2.2. Sample preparation

The solvent of the as received Nafion resin solution was evaporated at 60 °C to a solvent content of around 10 wt%. The Nafion solution containing 10 wt% of solvent was then diluted with a solvent mixture containing 4/1 wt ratio of methanol/water mixture. The solvent of the newly prepared Nafion solution was evaporated again at 60 °C and then followed by diluting with a methanol/water solvent mixture (4/1 wt ratio). The process was repeated five times. The final solution has a Nafion concentration of 10 mg/ml, which containing a solvent mixture of methanol/water (4/1 wt ratio). Finally, the 10 mg/ml Nafion solution was diluted with methanol/water solvent mixture (4/1 wt ratio) to various Nafion concentrations (ranging from 0.2 to 10.0 mg/ml) for membrane osmosis, viscoelasticity, and DLS measurements. The sample solutions for DLS and membrane osmotic pressure measurements were filtered through a 0.80 μm Millipore HWAP filter to remove dust. Those samples for viscoelasticity measurements were used directly without filtering.

2.3. Membrane osmosis

A Knauer membrane osmometer (Berlin, Germany) was used to carry out osmotic pressure π measurements. All the experiments were carried out at 30 °C.

2.4. Viscoelasticity analyzer

An oscillatory flow rheometer (Vilastic VE system, Vilastic Scientific Inc., Austin, Texas, USA) with a cylindrical tube of length 6.115 cm and inner diameter 0.0513 cm was used for dynamic viscoelasticity $G'(\omega)$ and $G''(\omega)$ measurements. The measurements were carried out at 30 °C.

2.5. Dynamic light scattering

The quasi-elastic light scattering was carried out with a

256-channel autocorrelator (Brookhaven Co, model BI9000) at 30 °C. The laser was a He–Ne ion (633 nm, operated at 20 mW, Spectra Physics model). The experiments were carried out at 30 °C with scattering angles of 30, 45, 60, 90, and 120°. To obtain the distribution of relaxation times, Eq. (1) a heterodyne data analysis method [20–24], was used to calculate field correlation function $g^{(1)}(t)$:

$$g^{(2)}(t) = 1 + \beta\{2X(1-X)g^{(1)}(t) + X^2[g^{(1)}(t)]^2\} \quad (1)$$

Where $g^{(2)}(t)$ is the intensity correlation function; $g^{(1)}(t)$ the field correlation function; X the homodyne ratio; and β the instrumental parameter. X can be obtained from Eq. (2):

$$X = 1 - [1 + \beta - g^{(2)}(0)]^{1/2}]/\beta^{1/2} \quad (2)$$

Where $g^{(2)}(0)$ is the value of $g^{(2)}(t)$ at $t \to 0$, and β can be obtained from the initial amplitude, $g^{(2)}(0)$, of polystyrene latex measurements [23]. In this study the β value is around 0.90. An inverse Laplace transformation (ILT) was made from $g^{(1)}(t)$ to obtain the distribution of relaxation times by using CONTIN software.

3. Results and discussion

3.1. Membrane osmosis

Membrane osmotic pressures of Nafion/methanol/water solutions with Nafion concentrations ranging from 0.2 to 10.0 mg/ml were measured at 30 °C using a Knauer membrane osmometer. Fig. 1 shows the plot of reduced osmotic pressure π/C versus Nafion concentration C. In a dilute θ-solution, the osmotic pressure π is proportional to the number of solute particles, and the slope of π/C versus C curve should be zero (i.e., second virial coefficient $A_2 = 0$). In a good solution, owing to the excluded volume effect, the slope of π/C versus C curve is positive (i.e., $A_2 > 0$). Fig. 1 shows that there are three Nafion concentration regimes, i.e. [Nafion] = 0.0–1.0 mg/ml, [Nafion] = 1.0–5.0 mg/ml, and [Nafion] = 5.0–9.0 mg/ml. As shown in Fig. 1, π/C decreases dramatically as Nafion concentration increases from 0.2 to 1.0 mg/ml. This result suggests that there is an aggregation (it is the secondary ionic aggregation as will be discussed in the following sections) of Nafion molecules as Nafion concentration is increased from 0.2 to 1.0 mg/ml, and the reduced solute particle number, i.e. n/C = [solute particle number]/[Nafion concentration], decreases with increasing Nafion concentration, leading to a reduction of π/C with increasing Nafion concentration. As Nafion concentration is higher than 1.0 mg/ml, π/C increases slowly from 1.0 to 5.0 mg/ml, indicating an increase in the reduced particle number of Nafion aggregation as Nafion concentration increases. As Nafion concentration is increased from 5.0 to 9.0 mg/ml, π/C decreases slowly with Nafion concentration, indicating another kind of Nafion aggregation occurs. These results suggest that the degree of Nafion aggregation is lower in the concentration range of 1.0–5.0 mg/ml than in the concentration ranges of 0.2–1.0 and 5.0–9.0 mg/ml.

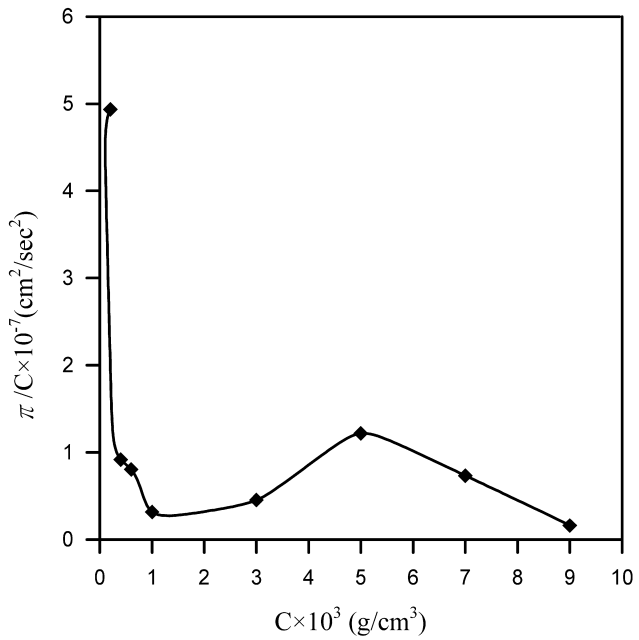

Fig. 1. Plot of reduced osmotic pressure π/C of Nafion/methanol/water solutions versus Nafion concentration C.

3.2. Depolarization ratio

For optically anisotropic molecules the polarization of the scattered light has components both parallel and perpendicular to the incident polarization. The anisotropic part of the scattering was expressed using depolarization ratio defined as follows [25]:

$$\rho_v = H_v(90°)/V_v(90°) \quad (3)$$

where the subscript v indicates measurements involving a vertically polarized incident laser light, $H(90°)$ the horizontally scattered light at the scattering angle $\theta = 90°$, and $V(90°)$ the vertically scattered light at the scattering angle $\theta = 90°$. For polyelectrolytes, which have electrostatic charge repulsion within the polymer chains, depolarization effects should not be neglected. The depolarization ratio is a function of polymer particle shape and anisotropy in solvent. This permits one to investigate the polymer shape and anisotropy [26,27]. The more anisometric the shape of a particle, the larger the optical anisotropy can be expected. Thus appreciable depolarization of scattered light, due to solute has been observed as rod like particles. On the other hand, for polymers with conformation of coils in solvents, the depolarization of scattered light, i.e. ρ_v, is quite low.

Table 1 summarizes ρ_v values of Nafion/methanol/water solutions with various Nafion concentrations. As shown in Table 1, ρ_v decreases slowly while Nafion concentration increases from 0.2 to 0.8 mg/ml. There is a dramatic

Table 1
ρ_v values of Nafion/methanol/water solutions

[Nafion] (mg/ml)	ρ_v
0.2	0.239
0.4	0.154
0.6	0.126
0.8	0.135
1.0	0.0175
3.0	0.0154
4.0	0.0129
5.0	0.0115
7.0	0.0103
9.0	0.0098

decrease in ρ_v as Nafion concentration is increased from 0.8 to 1.0 mg/ml. As Nafion concentration is higher than 1.0 mg/ml, $\rho_v < 0.02$ and decreases slowly with increasing Nafion concentration. These results suggest that there are anisometric rod-like particles in the solutions when Nafion concentration is lower than 1.0 mg/ml. The anisometric property decreases with increasing Nafion concentration. As Nafion concentration is higher than 1.0 mg/ml, the solution is close to optically isotropic. The ESR [15] and small angle scattering data [13,14] obtained from Nafion aqueous solutions have proposed that Nafion molecules aggregate and form anisometric rod-like particles through hydrophobic interaction of fluorocarbon backbone with sulfonic side chains locating at the interface of rod with solvent (Fig. 10(a) and (b)). These rod-like particles aggregate again through electrostatic attraction of ionic side chains and form larger and less anisometric clusters with solvent inside the center of the clusters [15]. It is obvious that at [Nafion] < 1.0 mg/ml, most of the Nafion molecules form rod like cylinder particles. Thus ρ_v value is larger than 0.1 when [Nafion] < 1.0 mg/ml. As Nafion concentration increases, more and more Nafion rod-like particles aggregate and form less anisometric secondary aggregation particles leading to a decrease in ρ_v value. When [Nafion] > 1.0 mg/ml, most of the Nafion molecules form less anisometric secondary aggregation particles and the solution system becomes isotropic with a ρ_v value much less than 0.1. Alderbert et al. [17] reported a dramatic decrease in reduced viscosities η_{red} of Nafion/methanol and Nafion/water solutions as Nafion concentration increases from 0.1 to 1.0 mg/ml, however, when Nafion concentration is above 1.0 mg/ml η_{red} decreases slowly with increasing Nafion concentration, indicating a 'polyelectrolyte effect' of dilute Nafion solution. The η_{red} data reported by Alderbert et al. are consistent with the present ρ_v data. The 'polyelectrolyte effect' is high at a Nafion concentration below 1.0 mg/ml and low as Nafion concentration is above 1.0 mg/ml.

3.3. Viscoelasticity

The viscoelasticity $G'(\omega)$ and $G''(\omega)$ of 0.2–9.0 mg/ml Nafion/methanol/water solutions were measured at 30 °C using an oscillatory flow rheometer. The slopes of $\log G'(\omega)$ and $\log G''(\omega)$ versus frequency $\log \omega$ at $\omega \to 0$ (i.e., $\omega < 100$ rad/s) were around 2 and 1, respectively, indicating a solution behavior. The storage modulus $\log \times G'(\omega)$ at $\omega = 10$ rad/s of each Nafion solution is taken and plotted against Nafion concentration and is shown in Fig. 2. The reduced storage modulus, i.e. $\log[G'(\omega)/C]$, at $\omega = 10$ rad/s is plotted against Nafion concentration and is shown in Fig. 3.

In a finite concentration sufficiently dilute polymer solution, $G'(\omega)$ can be expressed by Eqs. (4) and (5) [28]:

$$G'(\omega) = nkTF(\omega\tau, m_1, m_2) = (C/M_{agg})kTF(\omega\tau, m_1, m_2) \quad (4)$$

$$G'(\omega)/C = (n/C)kTF(\omega\tau, m_1, m_2) = (1/M_{agg})kTF(\omega\tau, m_1, m_2) \quad (5)$$

where n is the number of polymer aggregation particles per unit volume, k the Boltzman constant, T the absolute temperature, C the polymer concentration (mass per unit volume), and M_{agg} the mass of an aggregation particle. $F(\omega\tau, m_1, m_2)$ is a reduced function of $\omega\tau$, where τ is the relaxation time, and m_1 and m_2 the parameters depending on the shape and conformation of particles. From Eq. (5), it is obvious that $F(\omega\tau, m_1, m_2)$ and M_{agg} (or n/C) are the key factors controlling the value of $G'(\omega)/C$. If the degree of polymer aggregations or the shape and conformations of polymer aggregations does not change, the slope of $\log[G'(\omega)/C]$ versus C should be zero. The increase in degree of polymer aggregation causes an increase in M_{agg}, leading to a negative slope of $\log[G'(\omega)/C]$ versus C curve.

Fig. 2 shows that $G'(\omega)$ has a maximum value at [Nafion] $= 5.0$ mg/ml, indicating a transition of Nafion aggregation conformation. From Eq. (3), we know that either a decrease in n (or an increase in M_{agg}) or a decrease in $F(\omega\tau, m_1, m_2)$ causes a decrease in $G'(\omega)$. The decrease in

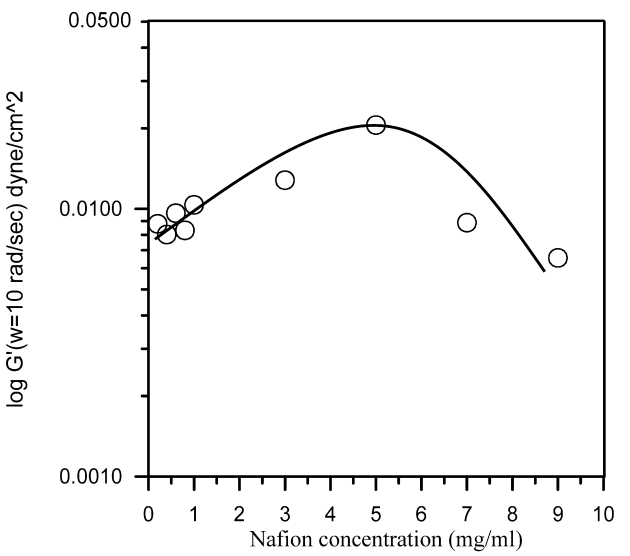

Fig. 2. Plot of storage modulus $\log G'(\omega)$ at $\omega = 10$ rad/s of Nafion/methanol/water solutions versus Nafion concentration C.

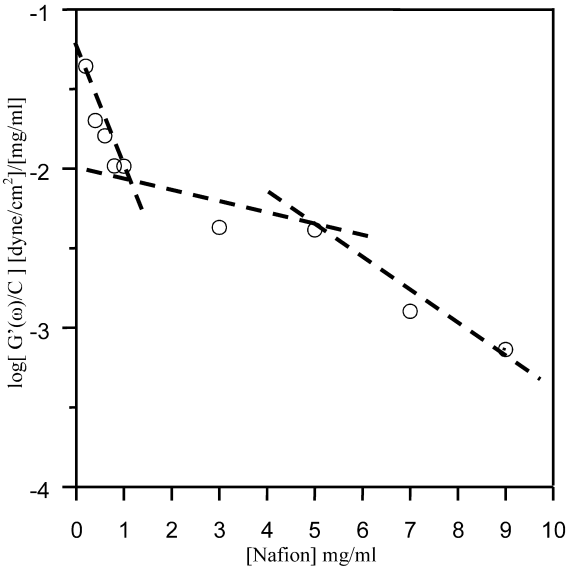

Fig. 3. Plot of reduced storage modulus $\log[G'(\omega)/C]$ at $\omega = 10$ rad/s of Nafion/methanol/water solutions versus Nafion concentration C.

$G'(\omega)$ as Nafion concentration increases from 5.0 to 9.0 mg/ml suggests the rod-like structure of Nafion aggregation particles become less elongated, due to the decrease in 'polyelectrolyte effect' as Nafion concentration increases.

Careful examination of the data shown in Fig. 3, we found three concentration regimes similar to those of Fig. 1 were observed, i.e. [Nafion] = 0.0–1.0 mg/ml, [Nafion] = 1.0–5.0 mg/ml, and [Nafion] = 5.0–9.0 mg/ml. The slopes of $\log[G'(w)/C]$ versus C in three Nafion concentration regimes are indicated by dashed lines. Fig. 3 shows that $[\log G'(\omega)/C]$ (at $\omega = 10$ rad/s) decreases dramatically while Nafion concentration increases from 0.2 to 1.0 mg/ml, and decreases slowly as Nafion concentration increases from 1.0 to 5.0 mg/ml, then decreases dramatically again when Nafion concentration increases from 5.0 to 9.0 mg/ml. These results are quite consistent with those of osmotic pressure measurements. Comparing the data of Fig. 1 with those of Fig. 3, we found that there are sharp negative slopes both in π/C and $\log[G'(\omega)/C]$ versus C data in Nafion concentration regimes of $C = 0.2$–1.0 and 5.0–9.0 mg/ml, indicating an increase in degree of polymer aggregation as Nafion concentration increases.

In the Nafion concentration regime of $C = 1.0$–5.0 mg/ml, the experimental data show a slight positive slope of π/C versus C and a slight negative slope of $\log[G'(\omega)/C]$ versus C. The positive slope of π/C versus C suggests that n/C increases (or M_{agg} decreases) with increasing Nafion concentration. In Section 3.4.1, DLS data reveals that the sizes of aggregation particles decrease as Nafion concentration increases from 1.0 to 5.0 mg/ml, indicating an increase in n/C as Nafion concentration increases. In Section 3.2, depolarization ratio measurements show $\rho_v \ll 0.1$ when [Nafion] $\geq$ 1.0 mg/ml, indicating that high ionomer concentration causes formation of less anisometric particles, i.e. the electrostatic shielding effect among the ionomers increases with increasing Nafion concentration leading to a reduction of effective charge density of Nafion molecules. Though n/C increases with concentration C, the reduction of charge density of Nafion molecules causes the formation of less elongated primary backbone aggregates leading to a slight negative slope of $\log[G'(w)/C]$ versus C as Nafion concentration increases from 1.0 to 5.0 mg/ml.

3.4. Dynamic light scattering

3.4.1. Dynamic light scattering from Nafion/methanol/water solutions

DLS from Nafion/methanol/water solutions were also carried out at 30 °C. Intensity–time correlation functions $g^{(2)}(t)$ were obtained from the measurements. Field correlation functions $g^{(1)}(t)$ were then calculated from $g^{(2)}(t)$ using Eqs. (1) and (2).

Fig. 4 shows the field correlation functions $g^{(1)}(t)$ (scattering angle $\theta = 30°$) versus $\log t$ for Nafion/methanol/water solutions with Nafion concentrations ranging

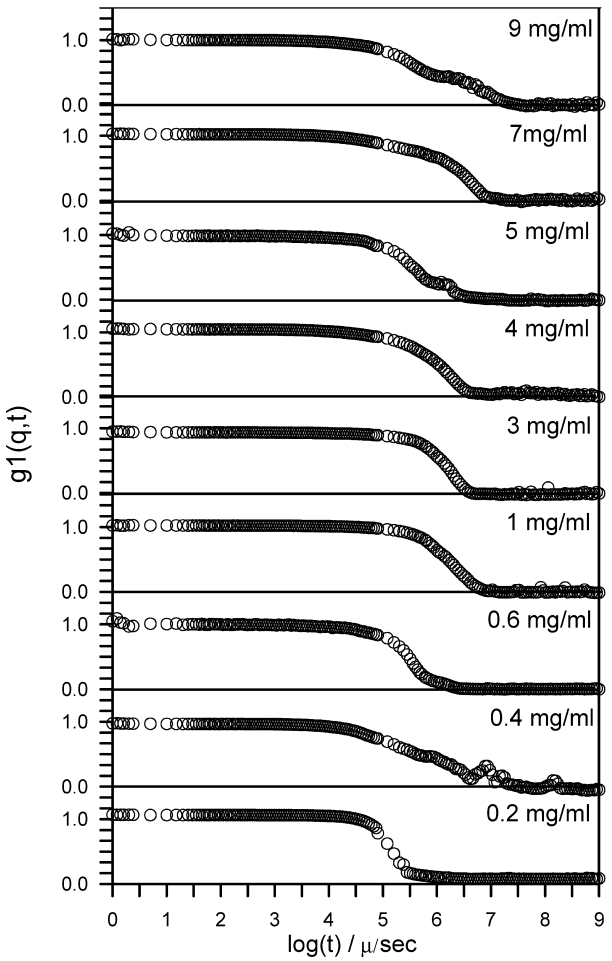

Fig. 4. Field correlation functions $g^{(1)}(t)$ (scattering angle $\theta = 30°$) versus $\log t$ of Nafion/methanol/water solutions with Nafion concentrations ranging from 0.2 to 10 mg/ml.

from 0.2 to 9.0 mg/ml. The correlation length ξ distributions obtained from CONTIN analyses are shown in Fig. 5.

As shown in Fig. 5, there are two modes of correlation length distributions with slow mode dominating the ξ distribution. From the results, we found that ξ increases from 2×10^3 to 2×10^4 nm as Nafion concentration increases from 0.2 to 1.0 mg/ml. When Nafion concentration increases from 1.0 to 5.0 mg/ml, ξ decreases slightly. When Nafion concentration is higher than 5.0 mg/ml, ξ increases with increasing Nafion concentration. These results are in agreement with those of membrane osmotic pressure π and dynamic viscoelasticity $G'(\omega)$ measurements. The particle size of 0.2 mg/ml Nafion in methanol/water solution, as shown in Fig. 5, is around 2×10^3 nm, which is larger than that of an ordinary polymer single chain. This datum suggests that even in a very dilute solution, there is an aggregation of Nafion molecules in methanol/water mixture solvents. SANS, SAXS, and ESR experiments have shown a rod-like structure of Nafion in aqueous solutions [13–15]. In these structures, the perfluoro backbones constitute the solvophobic core of the rods, and the ionic groups sit at the rod-solvent interface (Fig. 10(a)). In order to dissolve to the hydrophobic core of the rods, the higher hydrophobic solvents, i.e. propanol/water mixture solvent, was used to dissolve Nafion. DLS measurements were carried out from these solutions. These experimental data are shown in next section.

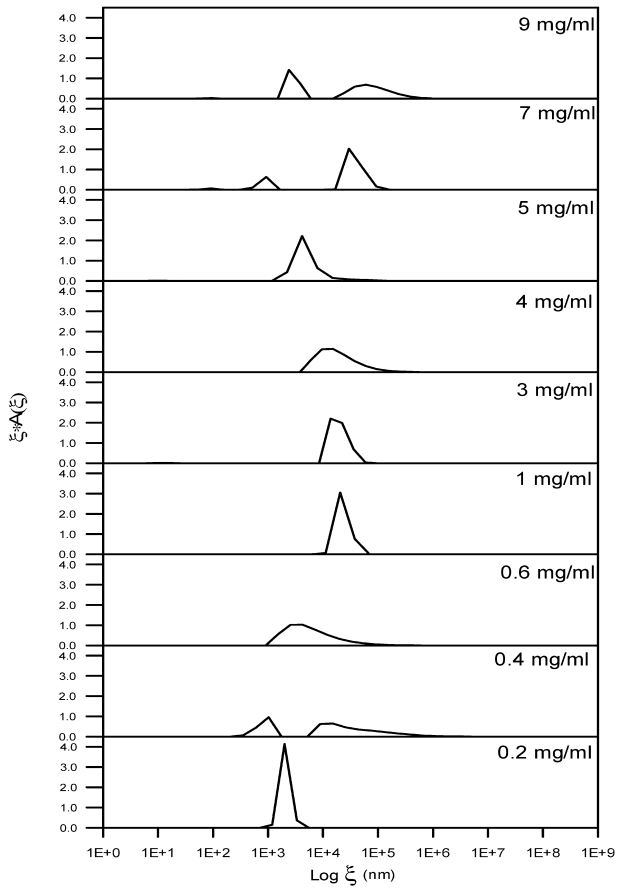

Fig. 5. Correlation length ξ distributions of Nafion/methanol/water solutions calculated from $g^{(1)}(t)$ data shown in Fig. 4.

3.4.2. Dynamic light scattering from Nafion/propanol/water solution

The cohesive energy density of Nafion has been determined experimentally from swelling measurements [6]. The results show that there are two distinct swelling envelopes corresponding to dual cohesive energy densities: one ($20.6\ J^{1/2}\ cm^{-3/2}$) is ascribed to the fluorocarbon backbone part of Nafion, whereas the other ($34.2\ J^{1/2}\ cm^{-3/2}$) is tentatively attributed to the side chain ion part in the material. In Table 2, we summarize the solubility parameters δ and dielectric constants ε of Nafion [6], water, methanol, ethanol, and propanol [29]. Table 2 shows that propanol has a better solubility with the fluorocarbon backbone of Nafion whilst methanol has a better solubility with Nafion ionic cluster part. The dielectric constant of the solvents decreases in the following sequence: water $<$ methanol $<$ ethanol $<$ propanol, indicating that the 'polyeletrolyte effect' of Nafion in various solvents decreases in the following sequence: water $<$ methanol $<$ ethanol $<$ propanol.

Fig. 6 shows the correlation length distribution of 0.4 mg/ml Nafion in propanol/water (in 4/1 wt ratio) at various scattering angles. The hydrodynamic radius is independent of scattering angle, indicating a diffusion process. The average hydrodynamic radius of Nafion in propanol/water solution is around 40 nm, which is a reasonable value for a single polymer chain. This result suggests that the Nafion primary aggregates in methanol/water mixture solvent are formed through hydrophobic perfluoro backbone aggregation rather than through side chain ionic aggregation while the Nafion concentration is lower than 0.4 mg/ml. This result is consistent with the model proposed from ESR [15] and small angle scattering data [13,14] obtained with Nafion aqueous solutions, which suggest that Nafion molecules aggregate through hydrophobic interaction of fluorocarbon backbone and form cylinder particles with ionic side chains located around the periphery of cylinders.

3.4.3. Dynamic light scattering from Nafion/methanol/water solution in the presence of NaCl

In order to study the ionic aggregation behavior of

Table 2
Solubility parameters and dielectric constants of Nafion, water, and alcohols

	δ ($J^{1/2}\ cm^{-3/2}$)	ε
Nafion	20.6	34.2
Water	47.9	78.4
Methanol	29.7	32.7
Ethanol	26.0	24.5
Propanol	23.5	19.9

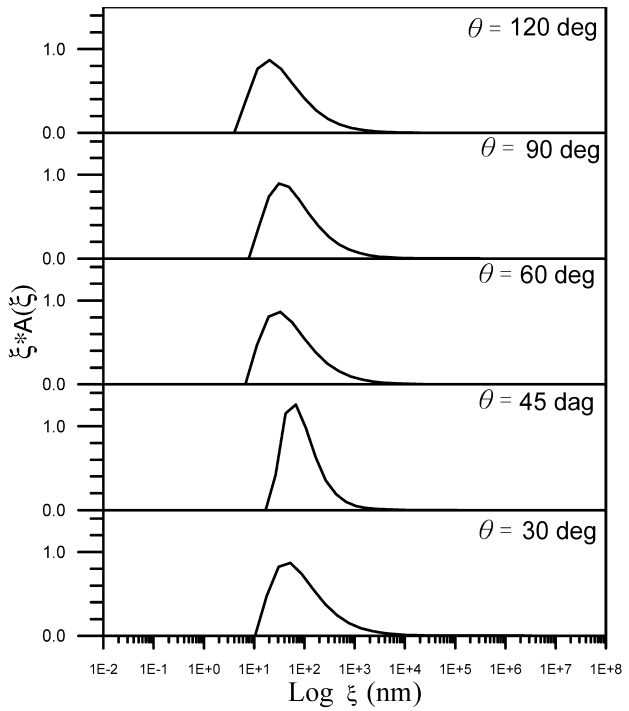

Fig. 6. Correlation length ξ distributions of 0.4 mg/ml Nafion/propanol/-water (in 4/1 wt ratio) at various scattering angles.

Nafion, NaCl was mixed into the solutions to observe the ionic shielding effect on the ionic aggregation phenomenon. Fig. 7 shows the correlation length distribution curves of 1 mg/ml Nafion/methanol/water solutions with and without the presence of 0.1 M NaCl, which were obtained from DLS at a scattering angle $\theta = 30°$. The data show that ξ of 1 mg/ml Nafion/methanol/water solution is around 2×10^4 nm and it is reduced to -2×10^3 nm while 0.1 M NaCl is mixed into the solution. The ξ value of 2×10^3 nm of 1 mg/ml Nafion/methanol/water solution in the presence of 0.1 M NaCl is similar to that of 0.2 mg/ml Nafion/mthanol/water solution without the presence of NaCl (Fig. 5, bottom). This result suggests that there is an ionic aggregation of Nafion in methanol/water mixture solvent as Nafion concentration is increased from 0.2 to 1.0 mg/ml. The primary particle size of Nafion in very dilute methanol/water solution is around 2×10^3 nm, which is an aggregation of Nafion molecules through solvophobic perfluoro backbones rather than through ionic side chains. These primary particles form larger secondary aggregated particles through ionic side chains.

Fig. 8 shows the correlation length distribution curves of 3 mg/ml Nafion/methanol/water solution with and without the presence of 0.1 M NaCl, which were obtained from dynamic light scattering at a scattering angle of $\theta = 30°$. For the solution without mixing with NaCl, DLS data show that ξ of 3 mg/ml Nafion/methanol/water solution is around 2×10^4 nm, and it is reduced to two modes of particle size distributions, i.e. 1×10^2 and 3×10^3 nm, when NaCl is mixed into the solution. These results suggest that there two different sizes of primary aggregation particles, which are formed through interaction of solvophobic perfluorocarbone backbone. The larger particles have similar particle sizes as that of 0.2 mg/ml Nafion/methanol/water solution (Fig. 10(a)), and the smaller particles are aggregates of several Nafion molecules through interaction of solvophobic perfluorocarbon backbones (Fig. 10(b)).

Fig. 9 shows the correlation length distribution curves of 7 mg/ml Nafion/methanol/water solution with and without the presence of 0.1 M NaCl, which were obtained from DLS

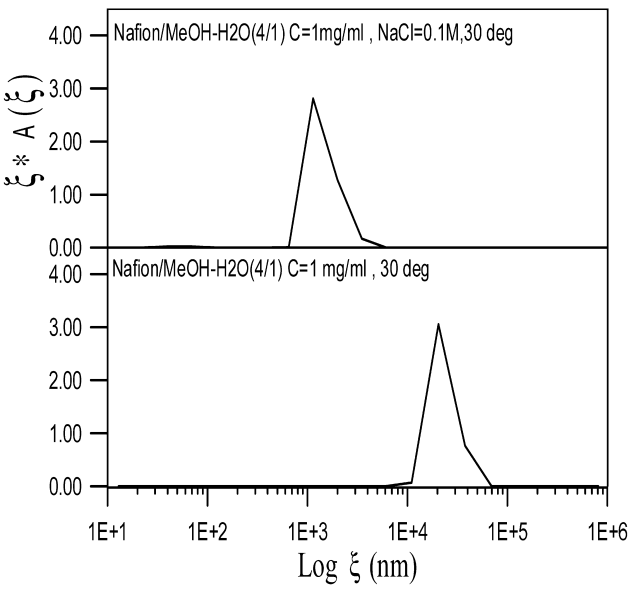

Fig. 7. Correlation length ξ distribution curves of 1 mg/ml Nafion/methanol/water solutions with and without the presence of 0.1 M NaCl. DLS scattering angle $\theta = 30°$. (top) 0.1 M NaCl; (bottom) 0.0 M NaCl.

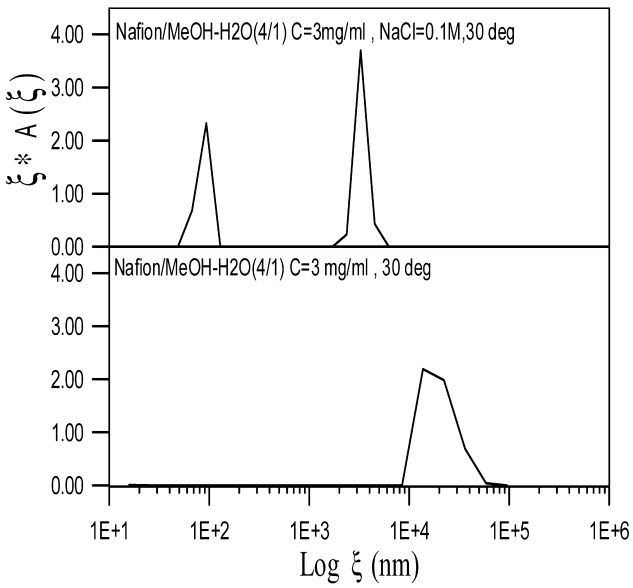

Fig. 8. Correlation length ξ distribution curves of 3 mg/ml Nafion/methanol/water solution with and without the presence of 0. 1 M NaCl. DLS scattering angle $\theta = 30°$. (top) 0.1 M NaCl; (bottom) 0.0 M NaCl.

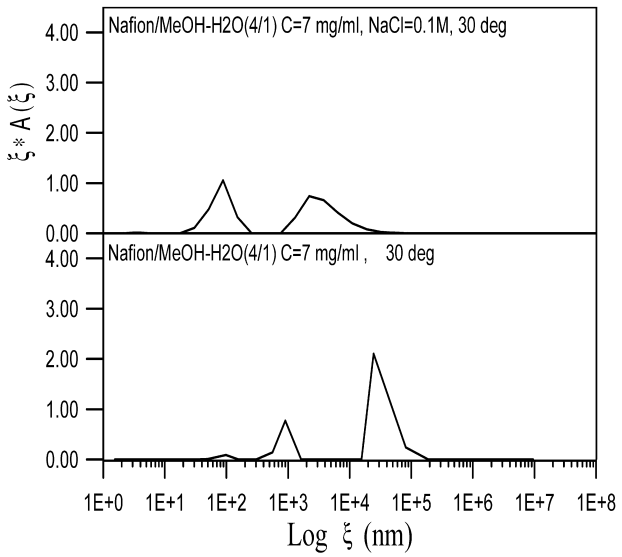

Fig. 9. Correlation length ξ distribution curves of 7 mg/ml Nafion/methanol/water solution with and without the presence of 0.1 M NaCl. DLS scattering angle $\theta = 30°$. (top) 0.1 M NaCl; (bottom) 0.0 M NaCl.

at a scattering $\theta = 30°$. For the solution without mixing with NaCl, DLS data show that there are two modes of particle sizes distributions with larger one located around 2×10^4 nm and smaller one located around 10^3 nm, the larger one dominates the particle sizes distribution. While 0.1 M NaCl was mixed into the solution, the aggregation particles were dissociated into two broad modes of particle sizes distributing around 3×10^3 and 8×10^1 nm. These results reveal that there are two different sizes of primary aggregation particles, which are formed through interaction of solvophobic perfluorocarbone backbone. The larger primary solvophobic aggregation particles have sizes of $\sim 2 \times 10^3$ nm. Its aggregation morphology is shown in Fig. 10(c) and will be discussed in Section 4. The smaller primary solvophobic aggregation particles (8×10^1 nm) have sizes similar to the smaller particles of 3 mg/ml Nafion/methanol/water/0.1 M NaCl solution (Fig. 10(b)). These particles sizes are little bit larger than that of Nafion single molecule (~ 40 nm), indicating a solvophobic aggregation of several Nafion molecules.

4. Discussion

The experimental results in present work are consistent with those reported from SANS, SAXS [13,14], and ESR study [15]. Those study reveals that Nafion backbones aggregate and form rod-like structures in aqueous solutions with ionic side chains located around the surface of the rods, in which the solvent-polymer contact is at the surface of the rods, rather than the open coil model, in which the solvent-polymer contact is maintained all along the polymer chain. At higher concentrations, these primary rod-like backbone aggregation particles will aggregate again through ionic side chains and form secondary ionic aggregations. Based on the experimental data, we propose an aggregation mechanism of dilute Nafion/methanol/water solutions. Fig. 10 shows the morphology of primary Nafion perfluoro backbone solvophobic aggregations in methanol/water mixture solvent in three dilute concentration regimes. While at a very dilute concentration of 0.2 mg/ml, the Nafion molecules aggregate through hydrophobic fluorocarbon backbones to form primary rod-like particles with ionic side chains located around the surface of the aggregation and a small amount of perfluoro backbone segments are located outside the rods (Fig. 10(a)). The disordered chain segments and ionic side chains are in contact with solvent. Since the solution is in a very dilute regime, the distance among the primary rod-like aggregation particles is far and no secondary aggregation of primary rod-like aggregation particles happens. As Nafion concentration increases from 0.2 to 1.0 mg/ml (i.e., C^*), the distance between the primary rod-like particles decreases and these rod-like particles aggregate through ionic side chains and form secondary ionic clusters with solvent inside the center of clusters [15]. The particle sizes of secondary ionic aggregation particles increase (Fig. 5) and reduced particle number n/C decreases (Figs. 1 and 3) as Nafion concentration increases from 0.2 to 1.0 mg/ml.

When [Nafion] $> C^* \sim 1.0$ mg/ml, depolarization ratio measurements show $\rho_v \ll 0.1$, indicating a low anisometric solution, i.e. most of the anisometric primary rod-like perfluoro backbone aggregation particles aggregate and form secondary ionic aggregation partcles, which are less anisometric. The electrostatic shielding effect among the ionomers increases with increasing Nafion concentration leading to a reduction of effective charge density of Nafion molecules and the primary rod-like aggregation particles will be less elongated. The part of disordered chain segments located outside the rods increases with increasing Nafion concentration. Some of the side chains, in which the ionic $-SO_3^-$ groups are shielded by counterions, may be embedded inside the core of perfluoro backbone aggregations, which causes steric hindrance for Nafion backbone to pack together. Thus the number and lengths of molecular chains incorporated in a rod decrease and the sizes of primary rod-like perfluoro backbone aggregation particles also decrease with increasing Nafion concentration. The smaller rod-like perfluoro backbone aggregation particle is shown in Fig. 10(b).

At a Nafion concentration between $C^* \sim 1.0$ mg/ml and $C^{**} \sim 5.0$ mg/ml, both rod-like perfluoro backbone aggregation particles shown in Fig. 10(a) and (b) may appear in the solutions, with the concentration of particle-b (Fig. 10(b)) increases and the concentration of particle-a (Fig. 10(a)) decreases as Nafion concentration increases. DLS data (Fig. 8) show that there are two modes of primary perfluoro backbone aggregation particle sizes distributions. Particles-a and particles-b may aggregate and form secondary ionic aggregation particles in the solution. Thus

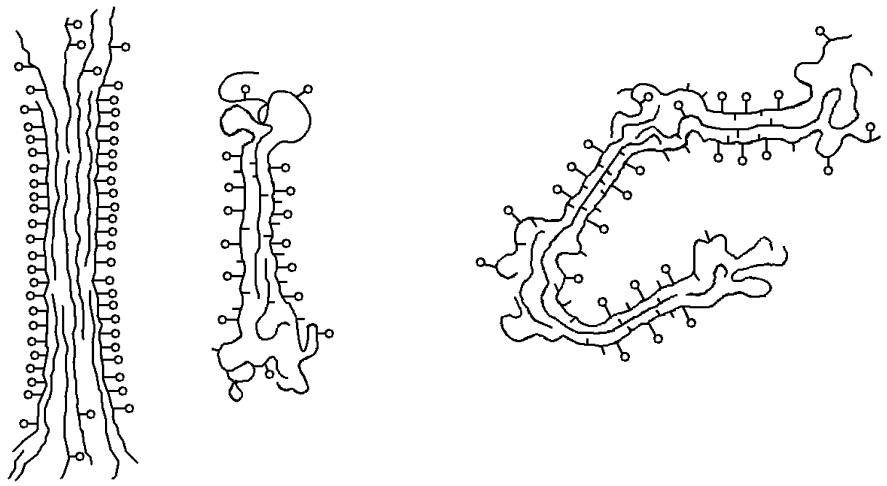

Fig. 10. The primary perfluoro backbone aggregations of Nafion in methanol/water mixture solvent. (~~) perfluoro backbone; (—O) side chain with effective ionic end group; (—) side chain with end group electrostatic shielded by counterions. (a) Highly elongated perfluoro backbone fringed rod-like aggregation particle, with high effective charge density ionic side chains located around the surface of the rod. (b) The effective charge density of ionic side chains is lower than that shown in (a). Some of the electrostatic shielded side chains are embedded in the core of rod-like structure and the number of molecular chains and the ordered chain segments embedded in the rod are less than that shown in (a). (c) The effective charge density of ionic side chains is lower than that shown in (b). More disordered chain segments are outside the rod. Some of the molecular chains may be incorporated into more than one rod and the disordered segments may overlap and self-assemble.

the size of secondary ionic aggregation clusters decreases (DLS data shown in Fig. 5) and the reduced particle number n/C increases (π/C data shown in Fig. 1) as Nafion concentration increases from 1.0 to 5.0 mg/ml.

As Nafion concentration is above $C^{**} \sim 5.0$ mg/ml, more disordered molecular chain segments are outside the rods of primary perfluoro backbone aggregation. Part of chain segments 'dangling' outside the rods becomes incorporated in other rods [15]. This process continues with increasing Nafion concentration and the disordered chain segments overlap and self-assemble (Fig. 10(c)). As Nafion concentration is between 5.0 and 9.0 mg/ml, both rod-like perfluoro backbone aggregation particles shown in Fig. 10(b) and shown Fig. 10(c) may appear in the solutions, with the concentration of particle-c (Fig. 10(c)) increases and the concentration of particle-b (Fig. 10(b)) decreases as Nafion concentration increases. DLS data (Fig. 9) show that there are two modes of primary perfluoro backbone particle sizes distributions. These two kind of rod-like perfluoro backbone aggregation particles, i.e. particle-b and particle-c, mix in the solution and aggregate to form secondary ionic aggregation particles. Thus the size of secondary ionic aggregation clusters increase (DLS data shown in Fig. 5) and the reduced particle number n/C decreases (π/C data shown in Fig. 1) as Nafion concentration increases from 5.0 to 9.0 mg/ml. The increase in disordered molecular chain segments and decrease in particle number n also cause a decrease in $G'(\omega)$ as Nafion concentration increases from 5.0 to 9.0 mg/ml (Fig. 2).

5. Conclusion

Two aggregation processes were observed in dilute Nafion/methanol/water solutions. Primary aggregation process causes the formation of smaller sizes ($\sim 10^3$ nm) aggregation particles, which can be dissociated into single molecular chains by dissolving Nafion in propanol/water mixture solvents, is attributed to the hydrophobic interaction of perfluoro backbone. The primary perfluoro backbone aggregations have a fringed rod-like structure, with the ordered chain segments incorporated in the rods, and the disordered chain segments are outside the rods. Secondary aggregation process causes the formation of larger aggregation particles ($\sim 10^4$ nm), which can be dissociated into primary aggregation particles by mixing NaCl salt into Nafion/methanol/water solutions, is attributed to the ionic aggregation of primary rod-like aggregation particles through electrostatic attraction of side chain $-SO_3^-$ ion pairs. Two critical concentrations were also observed, i.e. $C^* \sim 1.0$ mg/ml and $C^{**} \sim 5.0$ mg/ml, where transitions of Nafion aggregation conformations occur. C^* is the concentration at which most of the Nafion primary rod-like perfluoro backbone aggregation particles aggregate to form secondary ionic aggregations and the solution becomes isometric. At $C > C^*$, owing to the electrostatic shielding effect among the ionomers, the effective charge density of ionomers decreases with increasing Nafion concentration leading to a decrease in the content of ordered chain segments incorporated in rods and an increase

in the content of disordered molecular chain segments outside the rods. Thus the sizes of clusters decrease with increasing Nafion concentration while Nafion solution has a concentration between C^* and C^{**}. At concentrations above C^{**}, the disordered chain segments outside the primary rod-like aggregation particles start to overlap and self-assemble, thus the sizes of Nafion aggregation clusters increases with increasing Nafion concentration.

Acknowledgements

The authors would like to thank for the financial support by Energy Council of ROC (91-D0122) and Institute of Nuclear Energy Research, Atomic Energy Council of ROC (NS-90063).

References

[1] Grot WG. Nafion product bulletin. Wilmington, DE: Du Pont Co; 1986.
[2] Grot WG, Chadds F. European Patent 0066369; 1982.
[3] Heitner-Wiguin CJ. Membr Sci 1996;120:1.
[4] Wilson MS, Gottesfeld S. J Appl Electrochem 1992;22:1.
[5] Ren XM, Wilson MS, Gottesfeld S. J Electrochem Soc 1996;143:L12.
[6] Yeo R. Polymer 1980;21:432.
[7] Yeo SC, Eisenberg A. J Appl Polym Sci 1977;21:875.
[8] Roche EJ, Pineri M, Duplessix R, Levelut AM. J Polym Sci, Polym Phys Ed 1981;19:1.
[9] Gierke TD, Munn GE, Wilson FC. J Polym Sci, Polym Phys Ed 1981; 19:1687.
[10] Fujimura M, Hashimoto T, Hiromichi K. Macromolecules 1981;14: 1309.
[11] Redepenning J, Anson FC. J Phys Chem 1987;91:4549.
[12] Gebel G, Lambard J. Macromolecules 1997;30:7914.
[13] Alderbert P, Dreyfus B, Pineri M. Macromolecules 1986;19:2651.
[14] Loppinet B, Gebel G, Williams CE. J Phys Chem-B 1997;101:1884.
[15] Szajdzinska-Pietek E, Schlick S. Langmuir 1994;10(1101):2188.
[16] Li H, Schlick S. Polymer 1995;36:1141.
[17] Alderbert P, Grbel G, Loppinet B, Nakamura N. Polymer 1995;36: 431.
[18] Cirkel PA, Okada T, Kinugasa S. Macromolecules 1999;32:531.
[19] Jiang S, Xia KQ, Xu G. Macromolecules 2001;34:7783.
[20] Pusey PN, van Megen W. Physica A 1989;157:705.
[21] Joosten JGH, Gelade E, Pusey PN. Phys Rev-A 1990;42:2161.
[22] Joosten JGH, McCarthy JL, Pusey PN. Macromolecules 1991;24: 6690.
[23] Horkay F, Burchaard W, Hecht AM, Geissler E. Macromolecules 1993;26:3375. see also p. 4203.
[24] Horkay F, Burchard W, Geissler E, Hecht AM. Macromolecules 1993; 26:1296.
[25] Brookhaven Inc Corp. Instruction Manual for Model BI-2030AT Digital Correlator, New York: Brookhaven Instruments Corp; 1986.
[26] Kratochvil P. In: Huglin MB, editor. Light scattering from polymer solutions. London: Academic Press; 1972. Chapter 7.
[27] Kratochvil P. Classical light scattering from polymer solutions. Amsterdam: Elsevier; 1987.
[28] Ferry JD. Viscoelastic properties of polymers, 3rd ed. New York: Wiley; 1980. Chapter 9.
[29] Grulke EA. In: Brandrup J, Immergut EH, editors. Polymer handbook, 3rd ed. New York: Wiley; 1995. p. 519. Chapter VII.